

# Dissolution-Dynamic Nuclear Polarization with Rapid Transfer of a Polarized Solid

Karel Kouřil\*, Hana Kouřilová, Malcolm H. Levitt, and Benno Meier†  
School of Chemistry, University of Southampton, Southampton, SO17 1BJ, United Kingdom

(Dated: December 14, 2024)

We present a new method for preparing solutions with high degrees of nuclear spin polarization. The nuclear spins in the sample are polarized using conventional dynamic nuclear polarization (DNP) at a temperature of 1.5 Kelvin and a field of 6.7 Tesla. A bullet containing the frozen sample material is then ejected using pressurized helium gas, and shot into a receiving structure in a secondary 500 MHz magnet, where the bullet is retained and the polarized solid is dissolved rapidly. The transfer takes approximately 100 ms. A solenoid, wound along the entire transfer path is energized during the transfer to ensure adiabatic transfer and limit radical-induced low-field relaxation. The method offers a substantially faster transfer time than existing schemes, and is scalable towards small volumes while maintaining high concentrations of the target molecule. The drive gas is not mixed with the solvent thus suppressing foaming. Polarization levels of more than 20% have been observed for 1-<sup>13</sup>C-labeled pyruvic acid in solution.

Nuclear magnetic resonance (NMR) is a powerful, non-invasive analytical technique. It is broadly divided into two branches - NMR spectroscopy and magnetic resonance imaging (MRI). NMR spectroscopy provides structural and dynamic information of objects ranging from small molecules to proteins, while MRI provides spatial information with sub-millimeter resolution and has become indispensable for diagnostic medicine. The sensitivity of NMR however is very low [1], in particular because the interaction between nuclear spins and the applied magnetic field is orders of magnitude smaller than the thermal energy available at room temperature. Consequently, the nuclear spins are only weakly polarized. In thermal equilibrium at room temperature only 1 in 100,000 proton spins contributes to the signal that is recorded in an MRI scanner at 3 Tesla. Other nuclei exhibit a smaller gyromagnetic ratio, and hence an even smaller polarization. For example the polarization of the <sup>13</sup>C isotope of carbon at a given magnetic field is four times smaller than that of protons.

Dissolution-dynamic nuclear polarization (D-DNP), first described by Ardenkjær-Larsen and co-workers in 2003 [2], can increase the sensitivity of NMR by orders of magnitude. In D-DNP, a sample containing the molecule of interest is mixed with a suitable radical and polarized at a field of several Tesla and a temperature of approximately 1 Kelvin by transferring the substantially larger electron spin polarization to the nuclei using microwave irradiation. A jet of hot solvent, propelled by pressurized He gas, is then injected into the cryostat, dissolving the hyperpolarized substance. The hyperpolarized solution is flushed through a narrow transfer tube to the site of observation (an NMR or MRI instrument). The attainable signal enhancements of 10 000 and more are used in particular to detect human metabolism *in vivo* [3–5]. Hyperpolarized metabolites have potential uses in the monitoring of treatment response at early stages of cancer therapy [5–7].

Although notable applications of D-DNP to

biomolecules exist [8–11], it has not become a tool used routinely in NMR spectroscopy, despite important advances such as cross-polarization and microwave frequency sweeps that reduce the polarization time and yield polarization levels approaching unity [12, 13] in less than 30 minutes. This is in large part due to the way the hyperpolarized sample is dissolved and transferred. Solvent volumes of 3 mL or more are needed to prevent freezing in the cold regions of the polarizer, leading to a typically 100-fold dilution of the target molecule and a corresponding reduction in signal strength. The transfer of a liquid through a thin tube is intrinsically slow. Most instruments require up to 10s for sample transfer, and high-speed transfer systems employing pressurized HPLC loops still require 1 to 4s, often at the expense of even greater sample dilution [14, 15]. This is a substantial time compared to the spin-lattice relaxation time  $T_1$  with which the hyperpolarization decays, especially for larger molecules that exhibit shorter  $T_1$  values. Further problems are foaming caused by the propelling helium gas, and a low duty cycle, as the dissolution procedure typically transfers substantial amounts of heat into the sample space.

Here we show that these issues may be addressed collectively by transferring the sample rapidly in the solid state, and dissolving it only at the point of use. We thus overcome the current requirement to dissolve hyperpolarized samples in the polarizer, which is widely recognized as a major limitation of dissolution-DNP [16]. The two key advantages of extracting the sample in its solid form are scalability and speed. (i) Scalability. In conventional D-DNP the cryogenic sample environment rapidly cools the injected solvent, leading to blockages if solvent amounts of less than 3 mL are used. In rapid-transfer DNP only small solvent amounts are required since the solvent is never exposed to the cryogenic environment inside the polarizer. Here we use solvent amounts of 700  $\mu$ l to comfortably fill 5 mm NMR tubes. (ii) Speed. The transfer of a solid through a tube is very fast, even at

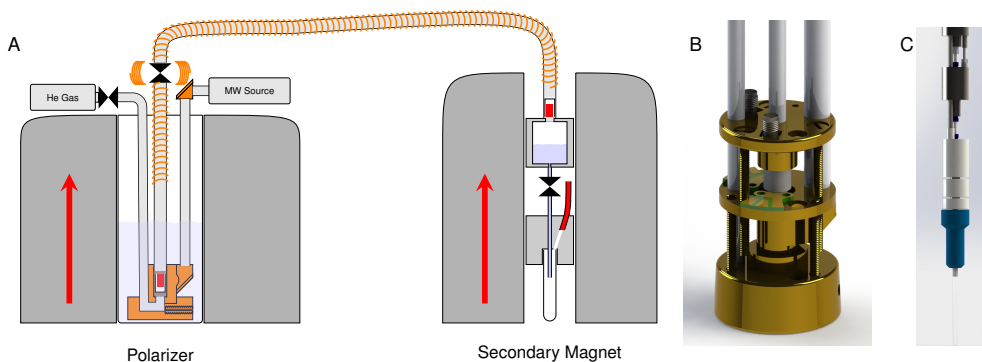


FIG. 1. Rapid transfer Dissolution-DNP equipment. (A) Sketch of the overall setup, comprising a polarizer magnet with cryostat and DNP insert, a transfer tube with a solenoid along its entire length, and an injection device inside a liquid-state NMR magnet. The polarity of the superconducting magnets is indicated by the red arrows. The direction of the applied pulsed magnetic field along the transfer changes at the valve, where two orthogonal pairs of Helmholtz coils are used to rotate the field. (B) Rendering of the lower part of the DNP insert showing the drive gas tube on the left, the main sample tube (center) and the microwave tube. The central brass piece hosts small circuitboards for tuning and matching. SMA connectors are soldered to the top brass piece that also pushes the coil support onto the bottom brass piece to seal the transfer path. (C) Rendering of the lower part of the injection device with a mounted NMR sample tube. The bottom of the solvent reservoir can be seen at the top of the image, followed by the pinch valve and a 3D printed nylon piece with an internal channel that connects a 3/16" steel tube to the NMR sample tube to facilitate evacuating the latter. Two further nylon pieces are screwed onto the NMR tube using a compression fitting, and facilitate a fast exchange of the NMR tube in between experiments.

moderate drive gas pressures.

The key challenge for a transfer in the solid state is to overcome fast relaxation at low field. In the present work this is achieved by rapidly transferring the sample and applying a carefully engineered pulsed magnetic field along the transfer path. We use this apparatus to transfer a sample of hyperpolarized 1-<sup>13</sup>C-pyruvic acid, which is the most widespread substance used in clinical studies.

## MATERIALS AND METHODS

The equipment for rapid transfer dissolution-DNP is shown in Fig. 1.

### Polarizer

The polarizer shares many elements with previously reported systems [2, 17], but the rapid sample ejection requires special consideration. Our DNP insert is mounted in an Oxford Instruments Spectrostat flow cryostat that is placed into a 6.7 Tesla magnet (Bruker). A KF50 pumping line connects the DNP insert to a 250 m<sup>3</sup>/h Roots pump, enabling temperatures down to 1.45 Kelvin. A rendering of the lower part of the DNP insert is shown in panel (B) of Fig. 1. The DNP insert comprises three steel tubes for (i) helium drive gas, (ii) sample insertion and ejection and (iii) microwave irradiation. The drive and sample tubes are 1/4" steel tubes with 4.2 mm ID, while the tube carrying the microwave is a 3/8" tube. All tubes were obtained from Wellington Tube Supplies Ltd.,

UK. The bottom of the DNP insert comprises three brass pieces. The bottom brass piece connects the drive tube with the sample tube. The channel is closed with a simple valve that is open during normal operation but closes during ejection of the sample. Thus during normal operation liquid helium flows into the sample tube for efficient sample cooling. During ejection the valve is closed by a small bead that is pushed against its opening by the drive gas. The center brass part carries a gold-plated mirror for the microwave irradiation and supports a printed circuit board for tuning and matching the radio-frequency (RF) saddle coil. The RF coil is wound onto a PEEK coil support that hosts the sample capsule. The sample capsules or bullets are made from teflon and can accommodate sample volumes up to 70  $\mu$ l. The PEEK piece is transparent for the microwave and RF fields required to polarize the sample and monitor the polarization level, but confines the helium gas inside the transfer path during sample ejection. Brass screws push the center brass piece onto the PEEK coil support that is thereby pushed onto the bottom brass piece. The sample tube fits into the top of the PEEK coil support that compresses on cooling, affording a good seal of the transfer path. A combination of standard RG-147 coaxial cable (RS Components Ltd, UK) and stainless steel coaxial cable (Aspen Electronics, UK) is used to connect the tuned and matched RF coil to an N-port on the top of the probe. The helium-level is measured using Allen-Bradley resistors and a home-built controller. The temperature inside the cryostat is measured using a Cernox sensor connected to an Oxford Instruments temperature controller. The top of the insert uses a KF50 6-way cross (Kurt J Lesker Ltd, UK)

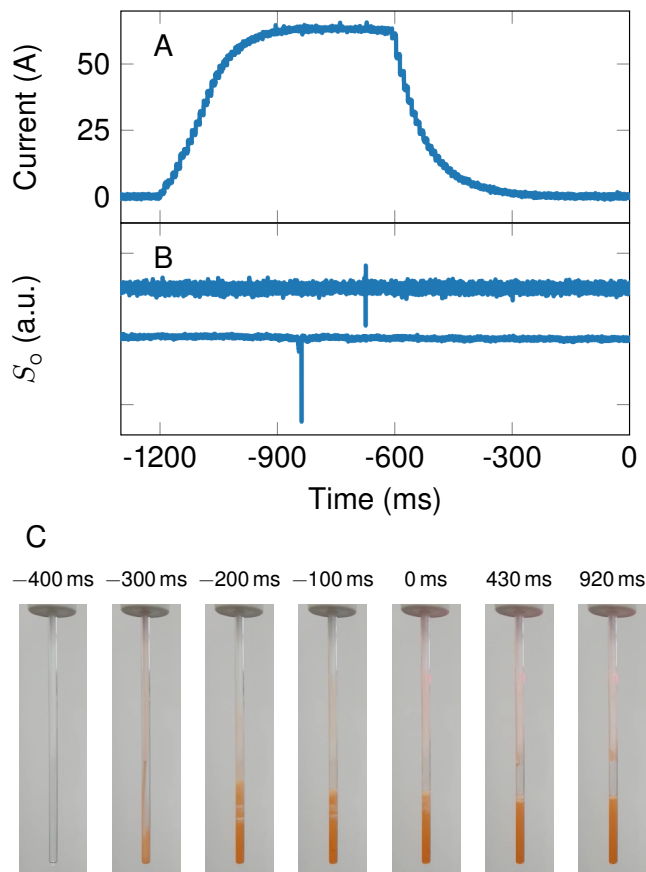


FIG. 2. Timing of the sample ejection, relative to the start of the NMR data acquisition at  $t = 0$ . At  $t = -1200$  ms the coil along the transfer path is energized. The voltage across the coil is ramped up to 200 V in approximately 150 ms. The current (panel A) takes approximately 200 ms to reach its maximum, and subsequently decreases slightly as the coils resistance increases due to resistive heating. At  $t = -900$  ms the sample ejection routine is started. The actuator chain comprises a mechanical relay, a pilot valve and an actuated plug valve, leading to a delay of another 100 ms before the bullet passes the first optical detector (panel B, bottom curve) near its start position. Approximately 100 ms later the bullet passes the second optical detector inside the second magnet (panel B, top curve), where the sample is dissolved in pre-heated solvent. At  $t = -500$  ms the pinch valve in the injector is opened, and the sample is sucked into an evacuated NMR tube. To demonstrate the loading of the NMR tube, a bullet containing 60  $\mu\text{l}$  of a 1:1 mixture of red dye and pyruvic acid was shot from the polarizer into the injection device that was preloaded with 700  $\mu\text{l}$  of degassed  $\text{H}_2\text{O}$ , heated to 50  $^\circ\text{C}$ . Selected frames from a video taken as the solution flows into the NMR tube are shown in panel (C). The time origin is the same as in panels A and B. The NMR acquisition is triggered at  $t = 0$ .

to connect the vacuum pump to the sample space and to connect the RF, Allen-Bradley and temperature cabling to the outside. A 1/4" inch T-union (Swagelok, UK) on top of the manual plug valve (SS-4P4T, Swagelok) at the

top of the sample tube is used to apply a small stream of helium gas when loading the sample capsule into the cold sample space, thereby preventing contamination of the system with air. After loading the sample, the 6 mm OD transfer tube (RS Components Ltd) is connected at the top of the Swagelok T-union. A 188 GHz, 50 mW microwave source (ELVA-1, Sweden) is connected to the top of the microwave tube.

### Sample preparation, loading and polarization

A 20 mM solution of OX063 trityl radical (Oxford Instruments, UK) in neat  $1\text{-}^{13}\text{C}$  pyruvic acid (Sigma Aldrich, US) was prepared. A volume of 10  $\mu\text{l}$  of this solution was pipetted into a 3.9 mm outer diameter, 10 mm long teflon bullet with a small concentric hole at the top to accommodate the solution. The capsule was immersed in liquid nitrogen to freeze the solution. The sample was then loaded into the sample tube of the DNP insert, whilst applying a small helium flow to prevent air ingress that could lead to blockages (the bullet is pushed past the helium inlet port using a short rod). The bullets are consumables, but are quickly made on a small lathe. After loading, the cryostat is filled with helium for approximately 20 min. Once the cryostat is full, the needle valve on the helium transfer line is closed and the temperature decreases to typically 1.5 K within 10 min, with a hold-time of up to four hours. The sample is polarized using microwave irradiation at 187.880 GHz, and the polarization buildup is monitored using a coil that is approximately tuned and matched to the  $^{13}\text{C}$  resonance frequency of 77.8 MHz.

### Transfer

Nuclear spin polarization relaxes rapidly at low field, in particular when the concentration of radicals is high [18, 19]. In the experiment presented here, the sample is shot through a 2.7 m long transfer tube that is connected to the top of the DNP insert and extends into the injection device in the secondary magnet. A solenoid wound along the entire transfer path is energized with a current of 60 A prior to sample ejection, using a 15 kW power supply (Keysight Technologies, US). A solenoid is also wound around the sample tube inside the polarizer, ensuring that the field experienced by the sample never drops below 75 mT. The solenoids are made by tightly winding 1 mm diameter insulated copper wire (RS Components Ltd, UK) onto the transfer tube, leading to an estimated field of 75 mT for a current of 60 A. The polarizer and the secondary magnet in our lab both have the same polarity. Therefore, a reversal of the field-direction along the transfer path is required. Any change in field direction should occur adiabatically, meaning that the Larmor

frequency  $\omega_L$  should always be substantially larger than the frequency of the rotation of the field as seen from a frame fixed with respect to the moving bullet [20]. In our setup, an adiabatic change of field direction is achieved using two pairs of Helmholtz-coils around the plug valve at the top of the sample tube. The individual coils have a diameter of approximately 10 cm. The first pair of Helmholtz coils is used to apply a transverse field, the second pair is a longitudinal anti-Helmholtz pair. Inside the polarizer the magnetic field is applied along the direction of travel. Following passage through the Helmholtz coils the magnetic field is applied opposite to the direction of travel. The field rotation is carried out over a distance of approximately 10 cm. At a bullet speed of 100 m/s this corresponds to a frequency of  $\sim 1$  kHz, well below the Larmor frequency  $\omega_L/(2\pi) = 800$  kHz of  $^{13}\text{C}$  at 75 mT. Note that the applied field of 75 mT also ensures that the Zeeman interaction dominates other spin interactions - the spins are quantized along the applied field at all times. In particular, the field is also sufficiently strong to prevent thermal mixing of the proton and carbon spins in the sample [18].

The passage of the bullet through the transfer tube is monitored using optical sensors [15] at the entrance and exit of the transfer tunnel. For the experiment described here, the drive gas pressure was set to 10 bar, leading to a transfer time of approximately 130 ms. Preliminary experiments show that the transfer time may be reduced to less than 70 ms at a drive gas pressure of 20 bar. The sample is only ejected after the transfer coil is fully energized. The time dependence of the current in the coil, and the signals from the optical detectors at the entry and exit of the tunnel are shown in Figs. 2A and B, respectively.

### Injection

Two different injection devices have been constructed. A simple device has been used for observations of quantum-rotor-induced polarization [21, 22]. It consists of a 3D printed receiver that connects to the NMR tube at the bottom, and to the transfer tube at the top. Inside the receiver a recession in diameter retains the sample capsule - the sample itself carries sufficient momentum to slide out of the capsule and into the NMR tube that is preloaded with solvent. A similar device has been described by Hirsch et al [19]. Venting slots at the top of the receiver provide an escape path for the pressurized helium gas. This device is fast and works well for organic solvents, but the impact of the sample on aqueous solutions often causes bubbles and leads to inhomogeneous solutions, in particular when using 5 mm NMR tubes.

We therefore constructed a new injection device, shown in Fig. 1 (C). In this device the sample capsule is also retained, but the sample itself is shot into a solvent reser-

voir located above the NMR tube. The solvent reservoir is machined from titanium and is equipped with a heater and a temperature sensor. With an internal diameter of 10 mm it facilitates fast dissolution and mixing without bubbles [10]. A 1/8" OD PTFE tube connects the solvent reservoir to a home-built valve in which a piece of silicon tubing is compressed with pressurized gas to block flow. The output of this valve is connected to an evacuated 5 mm NMR tube using a further piece of PTFE tubing. The valve opens upon releasing the pressure, and the solution is sucked from the solvent reservoir into the NMR tube. The evacuating line is closed to prevent boiling of the solution at low pressure. The filling of the NMR tube with aqueous solution is shown in Fig. 2(C). The tube is filled with solution at  $t = 0$  ms, approximately 860 ms after the bullet passes the optical sensor at the tunnel entrance inside the polarizer, and NMR acquisition is triggered. The first transient is recorded immediately, subsequent transients are recorded every second. Small remaining bubbles at the top of the sample collapse within the first second after the trigger.

### Control

The microwave source is controlled via a serial interface, directly from the computer. The Allen-Bradley resistors are excited and measured using a custom circuit, that interfaces to an Arduino microcontroller. A second Arduino controls a series of mechanical relays that switch 24V lines that in turn control pilot valves (SY3A00-5U1, SMC) that switch the various valves and the pneumatic actuator on top of the injection device. This Arduino also controls the temperature of the solvent reservoir of the injector. All Arduinos are controlled via ethernet. All control software on the computer is written in Python, software running on the Arduinos is written in C++.

## RESULTS

### Solid-state Polarization

The solid state polarization in our polarizer is estimated as  $47 \pm 10\%$ , based on a comparison of the hyperpolarized signal to the thermal signal measured at a temperature of 4.3 Kelvin. This polarization level is in the expected range for the polarization of neat pyruvic acid at 6.7 T and 1.5 K [23, 24].

### Liquid-state Polarization

The first two  $^{13}\text{C}$  NMR spectra of 10  $\mu\text{l}$  hyperpolarized 1- $^{13}\text{C}$ -labeled pyruvic acid, recorded after rapid transfer and dissolution in 700  $\mu\text{l}$  of degassed  $\text{D}_2\text{O}$ , are shown in

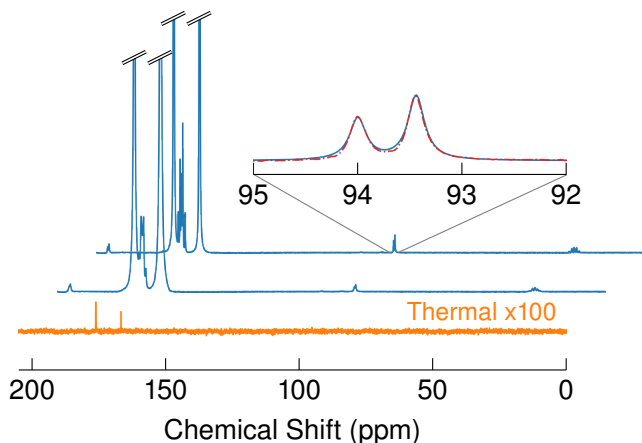


FIG. 3.  $^{13}\text{C}$  NMR spectra of hyperpolarized 1- $^{13}\text{C}$ -labeled pyruvic acid (blue lines) after rapid transfer and dissolution in degassed  $\text{D}_2\text{O}$ . The spectra show Fourier transforms of the first two transients recorded after dissolution. Each spectrum exhibits two strong peaks due to the presence of pyruvate and pyruvate hydrate. The inset is a close-up of the second hyperpolarized spectrum at approximately 94 ppm with the signal due to the natural abundance carbonyl of pyruvate hydrate. This signal is split into a doublet by the  $J$ -coupling to the (labeled) carboxyl carbon. The asymmetry in the doublet is modelled with two Lorentzians (red, dashed-dotted line) and yields an estimate for the  $^{13}\text{C}$ -polarization of  $21.7 \pm 1\%$ . The bottom, orange line shows a 100-fold magnification of the thermal equilibrium signal (64 transients averaged).

Fig. 3. The spectrum exhibits two strongly enhanced peaks that are due to the presence of pyruvic acid in both the oxo and the hydrated form [25]. As described previously [2], substantial polarization levels lead to an asymmetry in the doublet of nearby  $J$ -coupled spins. The inset of Fig. 3 shows a close-up of the doublet at 94 ppm, which is due to the natural abundance carbonyl carbon of pyruvate hydrate. The asymmetry of the doublet yields an estimate for the  $^{13}\text{C}$ -polarization of  $21.7 \pm 1\%$ .

The spectrum also shows a set of strongly enhanced peaks between the two main peaks at around 170 ppm. The origin of these peaks is currently unknown. They are not routinely observed in conventional dissolution-DNP, perhaps because they are associated with short-lived or rapidly-relaxing chemical intermediates.

## DISCUSSION

We have shown for the first time that it is possible to transfer solid hyperpolarized samples containing high concentrations of radical while retaining a substantial fraction of the nuclear spin polarization. Nevertheless we do lose a sizeable fraction of the spin polarization during transfer and dissolution. Preliminary data indicate that the polarization is best preserved at the highest transfer fields. The dependence of polarization transfer

efficiency (defined as the ratio of polarization in solution and in the solid state) on transfer speed is more difficult to ascertain since different drive pressures are likely to affect the sample temperature, and thereby the relaxation during the transfer. The sample may experience a modulation in transfer field on the 1 mm length scale of the coil winding. At a velocity of 100 m/s the frequency of this modulation approaches the Larmor frequency which may lead to faster relaxation at higher transfer speeds.

Numerous options exist to reduce polarization losses further. These include the (partial) use of permanent magnets to afford stronger transfer fields [26], and/or a cooling of the transfer path [19]. Polarization losses due to the presence of radicals may be reduced if the sample is divided into radical free parts and radical rich parts, although this approach has to date led to smaller polarization levels in solution [16]. Polarization losses may also be reduced if UV radicals are used to polarize the material [27].

Even without further optimization the approach presented here is attractive for a range of applications, in particular NMR spectroscopy, and imaging of small animals, where the amount of solution that can be used is often limited to 0.5 mL or less. The method does not suffer from foaming as the material does not get mixed with helium gas. The method does not involve moving parts, making it robust in practice. It may be combined with miniaturized NMR detectors [28, 29] which offer superior sensitivity for volume limited samples. The transfer in the solid phase also enables a combination of DNP with low-field thermal mixing [18]. Such a strategy does not suffer from the sample size limitations that exist for cross-polarization [12], and may lead to more strongly polarized substrates for applications spanning from spectroscopy to clinical research.

We would like to thank John Owers-Bradley and James Kempf for discussions. This research was supported by EPSRC (UK), grant codes EP/N002482, EP/M001962/1, EP/L505067/1, and EP/P009980 and the Wolfson Foundation.

Conflicts of Interest: BM, KK and HK are co-founders of Hyperspin Scientific Ltd, UK.

\* k.kouril@soton.ac.uk

† b.meier@soton.ac.uk

- [1] J.-H. Ardenkjaer-Larsen, G. S. Boebinger, A. Comment, S. Duckett, A. S. Edison, F. Engelke, C. Griesinger, R. G. Griffin, C. Hilty, H. Maeda, G. Parigi, T. Prisner, E. Ravera, J. van Bentum, S. Vega, A. Webb, C. Luchinat, H. Schwalbe, and L. Frydman, *Angewandte Chemie International Edition* **54**, 9162 (2015).
- [2] J. H. Ardenkjaer-Larsen, B. Fridlund, A. Gram, G. Hansson, L. Hansson, M. H. Lerche, R. Servin, M. Thaning, and K. Golman, *Proceedings of the National Academy of*

- Sciences **100**, 10158 (2003).
- [3] S. J. Nelson, J. Kurhanewicz, D. B. Vigneron, P. E. Z. Larson, A. L. Harzstark, M. Ferrone, M. van Criekinge, J. W. Chang, R. Bok, I. Park, G. Reed, L. Carvajal, E. J. Small, P. Munster, V. K. Weinberg, J. H. Ardenkjaer-Larsen, A. P. Chen, R. E. Hurd, L.-I. Odegardstuen, F. J. Robb, J. Tropp, and J. A. Murray, *Science Translational Medicine* **5**, 198ra108 (2013).
- [4] C. H. Cunningham, J. Y. Lau, A. P. Chen, B. J. Geraghty, W. J. Perks, I. Roifman, G. A. Wright, and K. A. Connelly, *Circulation Research* **119**, 1177 (2016).
- [5] V. Z. Miloushev, K. L. Granlund, R. Boltyanskiy, S. K. Lyashchenko, L. M. DeAngelis, I. K. Mellinshoff, C. W. Brennan, V. Tabar, T. J. Yang, A. I. Holodny, R. E. Sosa, Y. W. Guo, A. P. Chen, J. Tropp, F. Robb, and K. R. Keshari, *Cancer Research* **nil**, canres.0221.2018 (2018).
- [6] J. Kurhanewicz, D. B. Vigneron, K. Brindle, E. Y. Chekmenev, A. Comment, C. H. Cunningham, R. J. DeBerardinis, G. G. Green, M. O. Leach, S. S. Rajan, R. R. Rizi, B. D. Ross, W. S. Warren, and C. R. Malloy, *Neoplasia* **13**, 81 (2011).
- [7] K. M. Brindle, J. L. Izquierdo-García, D. Y. Lewis, R. J. Mair, and A. J. Wright, *Journal of Clinical Oncology* **35**, 2432 (2017).
- [8] H.-Y. Chen, M. Ragavan, and C. Hilty, *Angewandte Chemie* **125**, 9362 (2013).
- [9] G. Zhang, F. Schilling, S. J. Glaser, and C. Hilty, *Journal of Magnetic Resonance* **272**, 123 (2016).
- [10] G. Olsen, E. Markhasin, O. Szekely, C. Bretschneider, and L. Frydman, *Journal of Magnetic Resonance* **264**, 49 (2016).
- [11] J. Leggett, R. Hunter, J. Granwehr, R. Panek, A. J. Perez-Linde, A. J. Horsewill, J. McMaster, G. Smith, and W. Köckenberger, *Physical Chemistry Chemical Physics* **12**, 5883 (2010).
- [12] A. Bornet, R. Melzi, A. J. P. Linde, P. Hautle, B. van den Brandt, S. Jannin, and G. Bodenhausen, *J. Phys. Chem. Lett.* **4**, 111 (2013).
- [13] A. Bornet, J. Milani, B. Vuichoud, A. J. P. Linde, G. Bodenhausen, and S. Jannin, *Chemical Physics Letters* **602**, 63 (2014).
- [14] S. Bowen and C. Hilty, *Physical Chemistry Chemical Physics* **12**, 5766 (2010).
- [15] S. Katsikis, I. Marin-Montesinos, M. Pons, C. Ludwig, and U. L. Günther, *Appl Magn Reson* **46**, 723 (2015).
- [16] X. Ji, A. Bornet, B. Vuichoud, J. Milani, D. Gajan, A. J. Rossini, L. Emsley, G. Bodenhausen, and S. Jannin, *Nature Communications* **8**, 13975 (2017).
- [17] A. Comment, B. van den Brandt, K. Uffmann, F. Kurdzesau, S. Jannin, J. Konter, P. Hautle, W. Wenckebach, R. Gruetter, and J. van der Klink, *Concepts in Magnetic Resonance Part B: Magnetic Resonance Engineering* **31B**, 255 (2007).
- [18] D. T. Peat, M. L. Hirsch, D. G. Gadian, A. J. Horsewill, J. R. Owers-Bradley, and J. G. Kempf, *Physical Chemistry Chemical Physics* **18**, 19173 (2016).
- [19] M. L. Hirsch, N. Kalechofsky, A. Belzer, M. Rosay, and J. G. Kempf, *Journal of the American Chemical Society* **137**, 8428 (2015).
- [20] C. P. Slichter, *Springer Series in Solid-State Sciences* (1990), 10.1007/978-3-662-09441-9.
- [21] B. Meier, *Magnetic Resonance in Chemistry* **56**, 610 (2018).
- [22] B. Meier, K. Kouřil, C. Bengs, H. Kouřilová, T. C. Barker, S. J. Elliott, S. Alom, R. J. Whitby, and M. H. Levitt, *Physical Review Letters* **120**, 266001 (2018).
- [23] W. Meyer, J. Heckmann, C. Hess, E. Radtke, G. Reicherz, L. Triebwasser, and L. Wang, *Nuclear Instruments and Methods in Physics Research Section A: Accelerators, Spectrometers, Detectors and Associated Equipment* **631**, 1 (2011).
- [24] A. Kiswandhi, P. Niedbalski, C. Parish, S. Ferguson, D. Taylor, G. McDonald, and L. Lumata, *Magnetic Resonance in Chemistry* **55**, 828 (2017).
- [25] A. Lopalco, J. Douglas, N. Denora, and V. J. Stella, *Journal of Pharmaceutical Sciences* **105**, 664 (2016).
- [26] J. Milani, B. Vuichoud, A. Bornet, P. Miéville, R. Mottier, S. Jannin, and G. Bodenhausen, *Rev. Sci. Instrum.* **86**, 024101 (2015).
- [27] A. Capozzi, T. Cheng, G. Boero, C. Roussel, and A. Comment, *Nature Communications* **8**, 15757 (2017).
- [28] A. Webb, *Journal of Magnetic Resonance* **229**, 55 (2013).
- [29] G. Finch, A. Yilmaz, and M. Utz, *Journal of Magnetic Resonance* **262**, 73 (2016).